International Journal of Thermophysics, Vol. 20, No. 4, 1999

High-Temperature Containerless Viscosity Measurement by Gas-Film Levitation[1]

J.-Ch. Barbé,[2,3] C. Parayre,[2] M. Daniel,[2] M. Papoular,[4] and N. Kernevez[2]

The gas levitation process development program has, so far, been focused mainly on contact-free manipulation, on molding and shaping of liquids, on high-temperature contact-free treatment, and on shaping and solidification of interesting materials for scientific and technical purposes. Recently proposed by Parayre for viscosity measurements, this process eliminates the perturbing effects of the container, in particular, that of crystallization when studying supercooled liquids. The method consists of extracting viscosity values from the damped decay of perturbed liquid drops floating on a gas-film. An apparatus has been designed and developed for viscosity values higher than 1 Pa · s and at temperatures up to 2000°C. The method was applied to a silicate glass of industrial interest containing 70 wt% per cent of SiO_2, with viscosities ranging from 10^2 to 10^6 Pa · s. Experimental results are compared with the Vogel–Fulcher–Tamann law for viscosity predictions. This paper demonstrates the industrial and scientific interest of this new method for viscosity determinations, which can be used for the working and softening points of any glass. These results may lead to a better understanding of network-forming or network-modifying behavior in oxide glasses.

KEY WORDS: gas-film levitation; high temperature; oxide melts; viscosity.

1. INTRODUCTION

Sample levitation eliminates the use of containers and is appropriate for the measurement of temperature-dependent physical properties since it avoids the following problems related to the presence of a crucible:

[1] Paper presented at the Fifth International Workshop on Subsecond Thermophysics, June 16–19, 1998, Aix-en-Provence, France.

[2] Commissariat à l'Energie Atomique, DTA-CEREM, Grenoble 38041, France.

[3] To whom correspondence should be addressed.

[4] CRTBT, Centre National de la Recherche Scientifique and ESRF, Grenoble 38043, France.

0195-928X/99/0700-1071$16.00/0

- contamination of the melt by the crucible and
- solidification on the crucible wall when the melt is a mixture of solid and liquid phases.

Such methods, previously proposed and tested, placed the sample in levitation through various means, i.e., electromagnetic levitation [1], aerodynamic levitation [2], and aeroacoustic levitation [3].

Another method obtained by "gas-film levitation" was first described by Granier and Potard [4]. Based on the gas-film lubrication theory and developed for defect-free material synthesis, levitation is obtained by making a sample float on a thin gas film. In addition to rendering a crucible unnecessary, "gas-film levitation" can offer other advantages in viscosity determinations. For nonconducting materials, it is particularly suitable, compared to other methods, because of the possibility of both the use of medium weight samples (up to 200 g) and the presence of negligible perturbations on the forces acting on the drop. The viscosity determination then provides a measure of the intrinsic viscosity of the sample with unperturbed structure or microstructure, the only energy dissipation term being that of viscous dissipation.

A new method for measuring viscosity at high temperatures by "gas-film levitation" has been developed by Papoular and Parayre [5]. From the subsequent damping induced by an imposed perturbation on a drop in levitation, one determines the time constant of the periodic oscillation, which is in turn related to the viscosity of the drop.

The well-known dynamics of a viscous drop, and the underlying gas-film levitation viscosity measurements, was studied by Lamb [6], Basaran [7], Prosperetti [8], and Chandrasekhar [9]. The formulation gives expressions for the eigenfrequencies and the decay constants of the natural resonance of a spherical drop, and this was applied by Rodot et al. [10] to aerodynamic levitation.

Chandrasekhar defined a criterion to determine whether the shape fluctuations of the perturbed drop would follow a periodic oscillation or an aperiodic decay. This criterion depends linearly on the square of the viscosity. These two decay modes led Papoular and Parayre [5] to propose two methods to measure viscosity, one based on the periodic oscillation for low viscosities (<1 Pa $\cdot$ s) and the other on the aperiodic decay for high viscosities (>1 Pa $\cdot$ s).

The present paper is concerned with the second method, in which the viscosity is determined from the aperiodic decay of the perturbed drop. This method was applied to an industrial silicate glass (70 wt% SiO_2) whose viscosity ranges from 10^2 to 10^6 Pa $\cdot$ s; the first high-temperature (800 to 1200°C) viscosity measurements by "gas-film levitation" for this material are reported.

2. MOTION OF PERTURBED VISCOUS DROPS

A nearly *spherical viscous drop immersed in a region which has negligible dynamic effects* (a gas atmosphere) *and which fills the entire space* can be described by a superposition of spherical harmonics or Legendre polynomials with index (l, m),

$$r = R + \varepsilon Y_l^m(\vartheta, \varphi) \tag{1}$$

where R is the radius of the nonperturbed drop, is a function of time, and Y_l^m is a spherical harmonic. It can be assumed, for simplicity, that the surface maintains axial symmetry when an infinitesimal perturbation ε is applied. If $\varepsilon(t, \vec{r})$ is the local deformation, then one must always have $\varepsilon(t, \vec{r}) \ll R$.

For an incompressible fluid at low convection velocities, the motion of the perturbed surface obeys the linearized Navier–Stokes equations:

$$\begin{cases} \vec{\nabla} \cdot \vec{V} = 0 \\ \rho \dfrac{\partial \vec{V}}{\partial t} = -\vec{\nabla} p - \eta \vec{\nabla} \times (\vec{\nabla} \times \vec{V}) \end{cases} \tag{2}$$

where $\vec{V}$ is the velocity of the surface and ρ and η are the density and the dynamic viscosity of the fluid, respectively. Solutions to these equations must fulfill the following boundary conditions: (1) the radial component of the velocity must be compatible with the assumed form of the deformed boundary $\varepsilon(t, \vec{r})$, (2) the tangential viscous stresses must vanish at $r = R$, and (3) the (r, r) component of the total stress must vanish on the deformed boundary.

It is assumed that all parameters have the time dependence given by $\varepsilon_0 \exp(-(t/\tau))$.

Chandrasekhar's solution to the Navier–Stokes equations depends upon whether R is greater or less than a characteristic radius $R^* = \eta^2/\sigma\rho$, where σ is the surface tension, η is the viscosity, and ρ is the density of the material. If R is notably larger than R^*, the parameter τ is complex and the motion would be a periodic oscillation with an eigenfrequency ω_l and a damping time τ_l given by

$$\begin{cases} \omega_l^2 = \dfrac{\sigma}{\rho R^3} l(l-1)(l+2) \\ \tau_l = \dfrac{\rho R^2}{\eta} \dfrac{1}{(l-1)(2l+1)} \end{cases} \tag{3}$$

Thus when η is no longer negligible, the Kelvin modes, which are well known for inviscid drops, are damped with a mean lifetime τ_l.

If the drop radius is smaller than R^*, τ is real and the motion in this case is aperiodic, with a decay constant given by

$$\tau_l' = \frac{2(2l^2+4l+3)}{l(l+2)(2l+1)} \frac{\eta R}{\sigma} \tag{4}$$

This analysis can be applied to droplets in levitation which have a radius of a few millimeters. When the drop radius is smaller than the capillary length ($l_c = \sqrt{\sigma/\rho g}$) (water, 3.2 mm; AR-glas, 3.8 mm), the drop remains essentially spherical at equilibrium. For larger drops the equilibrium shape flattens out, the equatorial radius being of the order of the capillary length; one is then restricted to a certain range of form factor values (ratio between the equatorial and the polar radii). Room temperature tests have been performed to test the validity of the formulas for pseudo-spherical drops in levitation. For drops whose form factor is less than 1.3, the measured and the calculated decay constants for the aperiodic mode differ by only less than 10%. These results will be submitted for publication later.

Two modes can therefore be distinguished, the *periodic* and *aperiodic* modes. Henceforth, these two modes are referred to as such, and in either of them, the viscosity can be deduced from the above expressions from experimentally measurable quantities. One can cite typical cases to illustrate these modes. Water, whose drop radius is larger than R^* (10^{-8} m), would give rise to a periodic oscillation. On the other hand, for pure glycerol at room temperature ($\eta = 1.5$ Pa·s, $\rho = 1.25 \cdot 10^3$ Kg·m^{-3} and $\sigma = 63$ mN·m^{-1}), R^* and l_c would be about 1.5 cm and 2.2 mm, respectively; a small droplet a few millimeters in diameter would not be far from a spherical shape and would decay aperiodically. In this paper we have focused our attention on the "aperiodic" regime for viscosity measurement since details on the oscillation regime setup are given in Ref. 11.

3. EXPERIMENTAL PROCEDURES

3.1. Gas-Film Levitation

In view of the large viscosity range under study, two instruments have been developed, corresponding to each mode:

- a setup for the periodic mode applicable in the viscosity range of 10^{-3} to 1 Pa·s and

- a setup for the aperiodic mode applicable in the viscosity range above 1 Pa · s.

The setup for periodic oscillation has been sufficiently reported elsewhere [5] and is not described further here. The setup shown in Fig. 1 for the aperiodic mode is designed to perform four functions:

(1) to maintain a sample in levitation,

(2) to heat the sample and to ensure a temperature homogeneity,

(3) to impose a perturbation to the liquid sample, and

(4) to record measurable data.

The block diagram of the apparatus is presented in Fig. 2.

The sample is placed between two porous graphite membranes, the bearing and crushing membranes (Fig. 1), through which a pressurized gas is forced to create a laminar flow which maintains the sample in levitation by floating on a thin gas-film ($< 100\,\mu$m). Gas flow, regulated by controlling the difference between the argon pressure under the bearing graphite membrane and the argon atmosphere pressure around the sample,

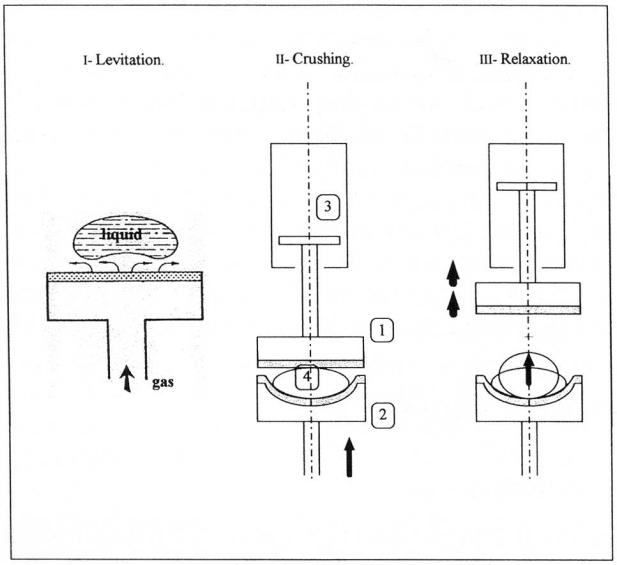

Fig. 1. Schematic diagram of levitated drop crushing technique: (1) crushing porous graphite membrane; (2) bearing porous graphite membrane; (3) hydraulic jack; (4) drop.

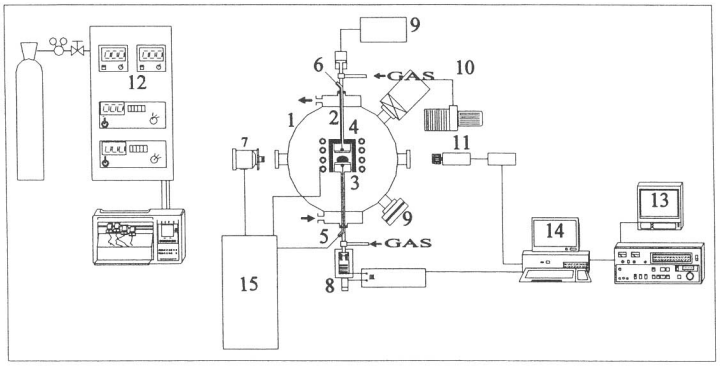

Fig. 2. Block diagram of the gas-film levitation viscosity measurement apparatus: (1) vessel; (2) crushing porous graphite membrane; (3) bearing porous graphite membrane; (4) susceptor; (5) thermocouple of regulation; (6) thermocouple of control; (7) pyrometer; (8) Schneeberger motion controller and motorized travel translation stage; (9) hydraulic jack; (10) vacuum generation; (11) Sony high-resolution color videocamera; (12) pressure regulation unit; (13) videocassette recorder; (4) computer for control of the motion controller; (15) Celes radiofrequency generator and temperature regulator.

results in very good stability of the sample's center of gravity. Initially, the sample is cast at a high temperature with a levitation overpressure. However, if there is no wetting and no chemical interaction between the sample and the porous graphite membrane, the sample can be directly cast in contact with the graphite, without levitation gas. After casting, gas flow is brought to normal measurement conditions and both thermal and mechanical equilibria are rapidly reached.

To obtain temperatures up to 2000°C, a Celes 50-kW and 100-kHz radiofrequency generator heats a graphite susceptor which eliminates electromagnetic perturbation on the sample. Low temperatures (<1500°C) are measured by thermocouples in contact with the two porous graphite membranes. Another measurement is obtained by focusing on the drop an Ircon two-color optical pyrometer with which two temperature ranges are possible, i.e., from 700 to 1500 and from 1000 to 3000°C. Below 1500°C, the temperature is regulated by the thermocouple on the bearing graphite membrane, while the second thermocouple and the pyrometer are used to control thermal homogeneity.

To introduce a perturbation, the drop at thermal and mecanical equilibrium is crushed between the two graphite porous membranes, through which gas is forced to avoid their contact with the sample. The crushing membrane is slowly brought near the droplet, and just as the droplet begins to deform, a crushing speed is imposed to reach the required

Table I. AR-Glas Composition

Component	Wt%
SiO_2	69.5
Na_2O	10.8
K_2O	5.3
CaO	7.8
Al_2O_3	4.2
B_2O_3	1.4

crushing amplitude. Crushing speed and amplitude are controlled by a Schneeberger motion controller and a motorized travel translation stage. Upon reaching the crushing amplitude, an hydraulic jack releases the crushing membrane and the drop begins, instantaneously, to relax. As the deformation amplitude is controlled by the motion controller, we know that the crushing amplitude uncertainty is lower than 0.03 mm. A geometrical uncertainty is encountered concerning the absolute position of the top of the drop with respect to the crushing membrane but this is estimated to be 0.1 mm.

With a Sony high resolution color videocamera and a Sony U-matic videocassette recorder, the upward relaxation of the perturbed drop is followed and recorded at 50 images per s until it has returned to its sessile form.

3.2. Application to an Industrial Glass

The procedure described above was applied to an industrial silicate glass, the AR-glass from Schott [12], whose composition is given in Table I. For each run, samples of about 380 mg were cast and the fixed experimental parameters were as follows.

- argon overpressure in the vessel, 50 ± 10 mbar;
- levitation overpressure, $\Delta P = 2 \pm 0.1$ bar;
- crushing speed, $200\,\mu\text{m} \cdot \text{min}^{-1}$; and
- the crushing amplitude, 1.4 ± 0.1 mm.

4. RESULTS AND DISCUSSION

4.1. Time Constant Determination

From the recorded data, the measurable quantity is the altitude of the top of the drop as a function of time during the relaxation. Since there

is uncertainty regarding the exact position of the top of the drop at the beginning of relaxation, the decay time constant is determined by fitting the experimental data to the following two-parameter exponential regression, which is justified if the assumptions of Chandrasekhar's analysis are satisfied, i.e., (1) the drop is nearly spherical, (2) the perturbation of the drop shape is infinitesimal, and (3) the deformation is relaxed by a pure ($l=2$) relaxation mode.

$$(z_{\text{inf}} - z(t)) = (z_{\text{inf}} - \times z_0) \times \exp\left(-\frac{\tau}{\tau_2}\right) \tag{5}$$

where $z(t)$ is the instantaneous altitude of the pole of the drop during relaxation, z_0 is the altitude of the pole of the crushed drop, and z_{inf} is the altitude of the pole of the sessile drop. For the AR-glas application, each sample mass of about 380 mg should give rise to a form factor of less than 1.2, which is within the range of form factor validity (<1.3) reported by Parayre and Dominguez [11] for low viscosities (20 Pa · s) at room temperature.

Equation (5) can be written in the form

$$\Delta h(t) = \Delta h_{\text{inf}} \times \exp\left(-\frac{t}{\tau_2}\right) \tag{6}$$

such that the two parameters of the regression become Δh_{inf} and τ_2.

A plot of the ratio $(\Delta h(t)/\Delta h_{\text{inf}})$ as a function of time reveals two behaviors depending upon the viscosity values. For "low" viscosities a single-exponential relaxation is found (Fig. 3a), while for high viscosities ($<10^4$ Pa · s) a slow decay precedes the final exponential relaxation (Fig. 3b). In the latter behavior, the initial slow decay may be the consequence of drop surface softening subsequent to sudden relaxation. Taking only the exponential relaxation into account for the case of high viscosities, the applicable regression relation would be the following three-parameter exponential law :

$$(z_{\text{inf}} - z(t)) = \Delta h_0 \times \exp\left(-\frac{t - t_0}{\tau_2}\right) \tag{7}$$

where t_0 refers to the start of exponential decay and $\Delta h_0 = z_{\text{inf}} - z(t_0)$.

A major problem is the increasing uncertainty in the time constant determination as the time constant value decreases which is the case for low viscosities (or high temperatures). However, this uncertainty never exceeds 30%.

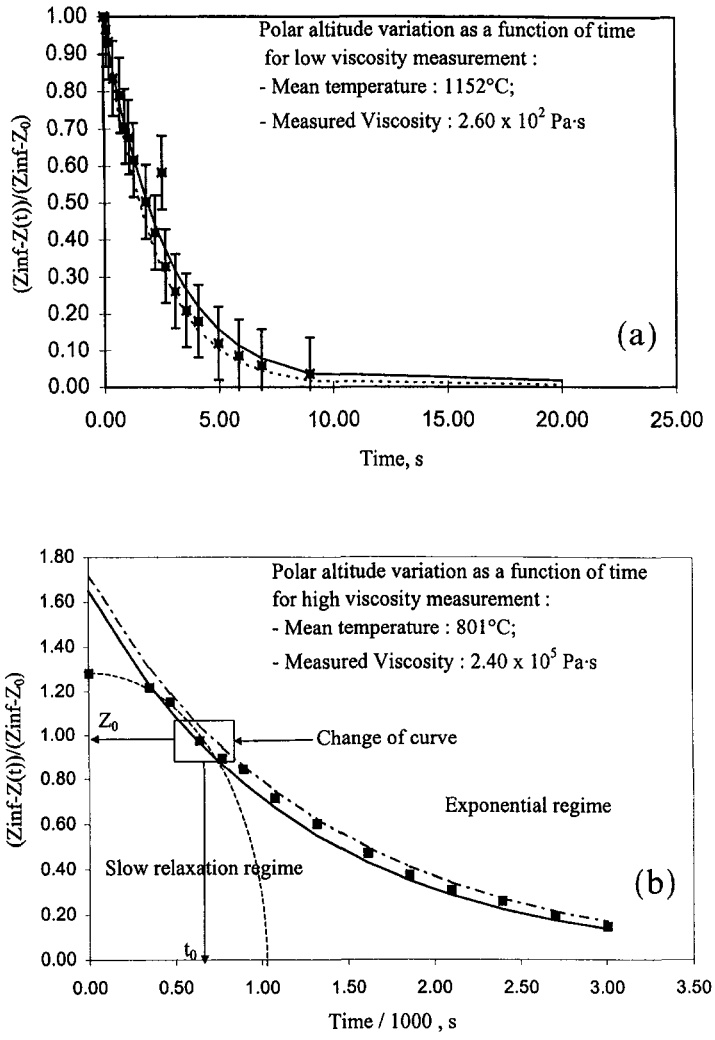

Fig. 3. (a) Exponential relaxation at low viscosity. (b) Slow relaxation regime at high viscosity before the exponential regime.

4.2. Discussion

Once the time constant for the decay is obtained, the viscosity value corresponding to the test temperature can be determined using Eq. (4) if the drop dimension, R, and the drop surface tension, σ, are known. The former can be obtained from experimental data and the latter calculated

Table II. Temperature Measurements and Calculated Surface Tension

Sample		Temperature (°C)				
Reference	Weight (mg)	T_b	T_c	T_p	T_m	σ (mN · m^{-1})
AR2.3	380	782	821	810	801	321.5
AR1.2	360	882	893	?	887	317.5
AR2.1	380	957	991	?	974	314
AR2.2	380	1035	1093	1130	1056	311
AR1.1	360	1098	1152	?	1125	308

from the sample composition by using the Dietzel, Lyon, and Appen coefficients [14] corresponding to the test temperature (see Table II). In these calculations, the test temperature is considered to be a mean of three experimental values, i.e., that of the bearing membrane, T_b, that of the crushing membrane, T_c, and that of the pyrometer, T_p. One notes that there can be a difference of about 30°C between the measured temperature values and their mean value and this may lead to a nonnegligible error on the calculated surface tension. However, one can estimate the probable extent of the error by the full variation of the surface tension in the studied temperature range [$\Delta\sigma = \sigma(800°C) - \sigma(1200°C) \approx 20$ mN · m^{-1}]; this represents less than 6,5% of the mean surface tension (310 mN · m^{-1}) in this range. The temperature variation between the crushing and the bearing membranes may reach 50°C at thermal steady state, but the surface tension variation would not be appreciable. Perturbing effects such as Marangoni convection or bulk natural convection can therefore be neglected.

The relaxation time constant and the viscosity values thus experimentally determined are presented in Table III; the total possible uncertainty in the determination is also indicated. The latter is taken as the sum of all possible experimental errors, i.e., in the determination of the surface tension, the drop radius, and the decay time constant.

Table III. Viscosity Measurements

Sample	T_m(°C)	Time decay (s)	Viscosity (Pa · s)	Uncertainty (%)
AR2.3	801	1500	1.4×10^5	25
AR1.2	887	100	9.3×10^3	25
AR2.1	974	20	1.8×10^3	35
AR2.2	1056	4.2	4.4×10^2	40
AR1.1	1125	2.5	2.6×10^2	35

The Vogel–Fulcher–Tamman (VFT) law [14] expresses the variation of viscosity as a function of temperature in the relation

$$\log(\eta) = A + \frac{B}{T - T_0} \tag{8}$$

where the coefficients A, B, and T_0 are calculated from the glass composition. Another set of coefficients can also be obtained by fitting this relation to viscosity values at the softening, the working, and the vitreous transition points of the glass as quoted by the manufacturer [12]. The VFT law is plotted in Fig. 4 for the two sets of coefficients, the solid curve corresponding to calculations from the glass composition, and the dashed curve obtained from fitting to manufacturer reference values.

The experimentally determined viscosity values are also shown in Fig. 4, and one finds that there is remarkably good agreement with the VFT law as calculated from the sample composition (solid curve). The agreement with the manufacturer's reference values, for which no estimate of uncertainty is available, may be slightly less but it remains satisfactory.

The Arrhenius VFT law describes a "strong glass" rheological behavior for high silica concentrations, which Angell [13] ascribes to a network-forming predominant oxide such as silica. In a "fragile glass," a network-modifying oxide such as CaO at present in sufficient concentrations to make the viscosity decrease much more rapidly as a function of temperature; the Arrhenius behavior is no longer valid. It should be noted

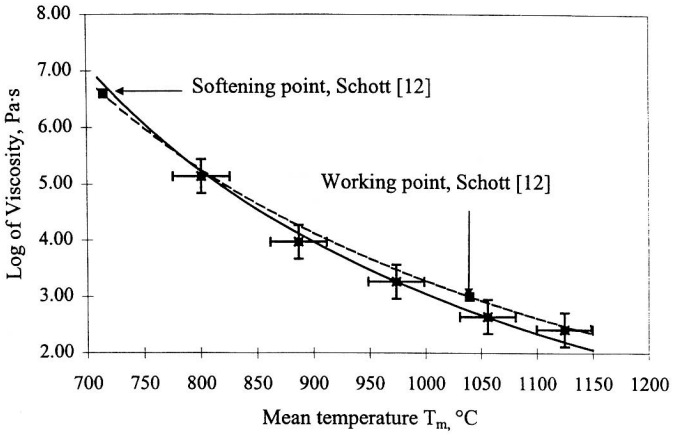

Fig. 4. Viscosity measurements: VFT viscosity calculations from the glass composition (solid line) and VFT calculations fitted from the industrial reference values (dashed line).

that the AR-glas composition is exactly in the validity range of the Lakatos coefficients [14].

5. CONCLUSION

A new container-free method for viscosity measurement, based on the damped motion of a liquid drop floating on a thin gas film and on the analysis of Chandrasekhar, has been proposed. An apparatus, appropriate for high viscosity values ($>1\,\text{Pa}\cdot\text{s}$) and a wide range of high temperatures (up to 2000°C), has been developed and described. The tests performed on an industrial silicate glass lead to very good agreement between experimentally determined values and the Vogel–Fulcher–Tamman law over a wide range of both viscosity (10^2 to $10^5\,\text{Pa}\cdot\text{s}$) and temperature (800 to 1150°C). This remarkable agreement also verifies Chandrasekhar's assumptions.

Viscosity determination by gas-film-levitation is a new and reliable technique suitable for conducting or nonconducting materials at high temperatures without the perturbing effect of a container. Its wide range of applicability for both viscosity and temperature is of industrial interest. Recent developments are being pursued and concern

(1) the improvement of thermal homogeneity in the vessel through thermal modeling as a continuation of previous numerical studies by Martin and Santailler [15];

(2) the possibility of reaching 2000°C, which will enable viscosity determinations in oxide melts for a better understanding of network-forming or network-modifying behavior in oxide glasses; and

(3) the automatic processing of the drop relaxation time constant determination.

REFERENCES

1. I. Egry and S. Sauerland, *Mater. Sci. Eng. A* **178**:73 (1994).
2. F. Babin, J.-M. Gagné, P.-F. Paradis, J.-P. Coutures, and J.-C. Rifflet, *Micrograv. Sci. Technol.* **VII**:283 (1995).
3. P. C. Nordine and J. K. R. Weber, *Micrograv. Sci. Technol.* **VII**:279 (1995).
4. J. Granier and C. Potard, *Proc. 6th Eur. Symp. Mater. Sci. Micrograv.*, Bordeaux, France, ESA SP-256 (1987).
5. M. Papoular and C. Parayre, *Phys. Rev. Lett.* **78**:2120 (1997).
6. H. Lamb, *Hydrodynamics* (Cambridge University Press, Cambridge, 1932).
7. O. A. Basaran, *J. Fluid. Mech.* **241**:169 (1992).
8. A. Prosperetti, *Proc. Colloq. Drops Bubbles*, Vol. 2 (1974), pp. 357–370.
9. S. Chandrasekhar, *Hydrodynamic and Hydromagnetic Stability* (Clarendon Press, Oxford, 1961), pp. 466–480.

10. H. Rodot, A. Lasek, and C. Bisch, *Méc. Théor. Appl.* 1:165 (1982).
11. C. Parayre and G. Dominguez, *Note Technique DEM/SPCM No. 14/96* (CEA, Grenoble, France, 1996).
12. Schott, *Industrial Glasses*, Product Information No. 40001[e].
13. C. A. Angell, *Science* **267**:1924 (1995).
14. H. Scholtze, *Institut du Verre de Paris* (Paris, 1980).
15 V. Martin and J.-L. Santailler, *Compte Rendu DEM/SPCM No. 98/06* (CEA, Grenoble, France, 1998).